Am J Cancer Res 2022;12(1):48-67
www.ajcr.us /ISSN:2156-6976/ajcr0115628

Original Article

Mitochondrial DHODH regulates hypoxia-inducible factor 1 expression in OTSCC

Wei Gao[1*], Lingyin Hu[1*], Minjuan Zhang[1], Shuai Liu[1], Shaowei Xu[2], Velda Ling-Yu Chow[1], Jimmy Yu-Wai Chan[1], Thian-Sze Wong[1]

[1]Department of Surgery, LKS Faculty of Medicine, The University of Hong Kong, 21 Sassoon Road, Pokfulam, Hong Kong, China; [2]Department of Head and Neck Surgery, Cancer Hospital of Shantou University Medical College, 7 Raoping Road, Shantou 515031, Guangdong Province, China. [*]Equal contributors.

Received June 4, 2020; Accepted August 15, 2021; Epub January 15, 2022; Published January 30, 2022

Abstract: Oral tongue squamous cell carcinoma (OTSCC) was one of the most hypoxic tumors with unfavorable outcomes. Hypoxia-inducible factor-1 (HIF-1) signaling was associated with cancer proliferation, lymph node metastasis, angiogenesis and poor prognosis of OTSCC. Dihydroorotate dehydrogenase (DHODH) catalyzed the rate-limiting step in the de novo pyrimidine biosynthesis. The aim of the study was to explore the biological function of DHODH and investigate whether DHODH regulated HIF-1 signaling in OTSCC. Proliferation, migration and anoikis resistance were used to determine the function of DHODH. Western blot and luciferase activity assays were used to determine the regulatory role of DHODH on HIF-1. We found that increased DHODH expression was associated with advanced tumor stage and poorly differentiated tumor in head and neck cancer patients in The Cancer Genome Atlas (TCGA). DHODH enhanced the proliferation and aggressiveness of OTSCC. Moreover, DHODH prompted tumor growth and metastasis *in vivo*. DHODH promoted transcription, protein stability, and transactivation activity of HIF1A. DHODH-induced HIF1A upregulation in OTSCC can be reversed by reactive oxygen species (ROS) scavenger, indicating that DHODH enhanced HIF1A expression via ROS production. DHODH inhibitor suppressed DHODH-mediated ROS generation and HIF1A upregulation. Targeting DHODH using clinically available inhibitor, atovaquone, might provide a new strategy to treat OTSCC.

Keywords: OTSCC, HIF1A, DHODH, ROS, atovaquone

Introduction

Oral tongue squamous cell carcinoma (OTSCC) is a major form of head and neck cancers developed from the stratified layer of mucosal linings. Approximately, the annual number of new cases is 300,000 worldwide [1]. Remarkable high prevalence is observed in Asia countries. In Hong Kong, increasing incidence is observed. OTSCC is commonly found in the anterior two-thirds of the tongue, the tonsillar region, the buccal mucosa, the gingiva, and the lips [2]. Prognosis of oral cancer remains poor, with 5-year survival rates around 50% [2]. Apart from uncontrolled growth, lymph node metastasis and recurrence are common features presented by OTSCC patients [3]. Tobacco and alcohol consumption are major external risk factors for oral cancers. Target treatment regime for OTSCC remains limited [4]. There are no effective preventive measures for OTSCC. Given the increasing incidence, there is a pressing need to delineate the molecular mechanisms underlying OTSCC tumorigenesis.

OTSCC is one of the most hypoxic tumors with unfavorable outcomes [5]. Intra-tumoral hypoxia refers to the low oxygenation (PO_2<10 mm Hg) in the primary tumour due to the poor vasculature development for oxygen delivery during cancer progression. Normal cells will stop to proliferate under oxidative stress. In contrast, cancer can adapt to survive and grow by upregulating the master oncoprotein, hypoxia-inducible factor-1 (HIF-1). HIF-1 protein is a heterodimeric transcription factor containing basic-helix-loop-helix proteins. About 1-1.5% genome includes genes that are transcriptionally responsive to hypoxia [6]. HIF-1 is a heterodimer composing of HIF1A and HIF1B. HIF1B is

constitutively expressed, and HIF1A degrades rapidly at the condition with sufficient oxygen supply. Under the hypoxic state, HIF1A will accumulate quickly in the cells and form dimer with HIF1B to form functional HIF-1 protein. HIF-1 signaling plays a crucial role in cancer proliferation, lymph node metastasis, epithelial-mesenchymal transition, glycolytic metabolism, and poor prognosis of oral cancers [7-9]. Further, HIF1A accumulation is associated with angiogenesis and intratumoral lymphatic density of lower lip squamous cell carcinoma [10, 11].

Reactive oxygen species (ROS) are reactive oxygen-containing molecules produced in the course of oxygen metabolism. As a major organelle responsible for oxidative metabolism, mitochondria are a key intracellular ROS generator in both normal and cancerous epithelial cells. ROS can activate key cancer singling cascades, including ERK1/2, JNK/MAP kinase, and PI3K/Akt [12, 13]. ROS level is remarkably increased in cancer cells at both normoxic and hypoxic conditions. Hypoxic cells showed a remarkable increase in the HIF-1 level. Meanwhile, the ROS level increased in parallel [14]. ROS is produced from the electron transport chain when the oxygen level reduces, and mitochondria potential decreases [15]. It is speculated that the mitochondria complex III is the major ROS producer when the cell is exposed to a low oxygen environment [15]. ROS generated in the hypoxic cell can increase HIF-1 activity by inducing HIF1A transcription [14]. Increasing evidence supported that the oxygen level is not the only regulator on HIF-1. Activation of particular oncogenic singling pathways can result in HIF-1 expression in cancers at the normoxic condition. As high oxidative stress is a general feature of human cancers, we speculated that key ROS-producing enzyme is involved in the transcription upregulation of HIF1A in both oxygen-dependent and -independent conditions.

Dihydroorotate dehydrogenase (DHODH) located on the inner mitochondria membrane controls the rate-limiting step in the de novo pyrimidine (nitrogen base) biosynthesis. DHODH catalyzes the conversion of dihydroorotate (DHO) to orotate by transferring electrons to ubiquinone [16, 17]. Pyrimidine derivatives are essential constitutes (uracil, thymine & cytosine) of RNA/DNA [18]. DHODH activity is particularly important for rapidly proliferating cancer cells and tumor growth. By analyzing expression data in the Cancer Genome Atlas Project (TCGA), we found that DHODH overexpression is significantly associated with the clinicopathological parameters of head and neck cancer patients. DHODH-regulated pyrimidines synthesis could trigger responses of transcription factor p53 [17]. Apart from pyrimidines synthesis, new data suggesting that DHODH activity will affect the reactive oxygen species content in cancers cells [19]. DHODH is physically associated with respiratory complexes II and III [18]. The existing evidence suggests that DHODH might have a function to control cellular gene expression or signaling pathways. Additionally, we speculated that DHODH-mediated ROS is playing an active role in the process. However, the role of DHDOH in ROS-generation in OTSCC remains unclear.

In this study, we reported that DHODH has a tumor-promoting function in OTSCC. Increased DHODH expression increases the proliferation and aggressiveness of OTSCC. Moreover, we found that the DHODH-associated ROS generation is associated with the transcription activity of HIF-1 in OTSCC. DHODH regulates HIF-1 activity by promoting HIF1A expression at the transcription level. In mouse xenograft, DHODH upregulation is linked with increased nuclear HIF-1 staining in the OTSCC. Moreover, we noticed that clinical DHODH inhibitor is useful to suppress DHODH-mediated ROS generation and HIF1A upregulation. These data suggest that targeting DHODH is a potentially useful approach which inhibits the tumorigenicity of OTSCC by suppressing the ROS-mediated HIF-1 increase at both normoxic and hypoxic condition.

Materials and methods

Cell culture

CAL27 was a tongue squamous cell carcinoma cell line obtained from ATCC. SAS was a tongue squamous cell carcinoma cell line obtained from JCRB cell bank. CAL27 cells were maintained in RPMI-1640 medium (Gibco, MA, USA) with 10% Fetal Bovine Serum (FBS, Gibco) and 1% Antibiotic-Antimycotic (Gibco). SAS cells were cultured in Dulbecco's modified Eagle's medium/Ham's F12 medium (DMEM/F12, Gibco) with 10% FBS (Gibco) and 1% Antibiotic-

Antimycotic (Gibco). All the cells were incubated at 37°C under 5% CO_2 environment in a humidified incubator.

siRNA transfection

CAL27 and SAS cells were transfected with DHODH-siRNA-1 (15 nM, QIAGEN, CA, USA) or DHODH-siRNA-2 (15 nM, QIAGEN) or negative control siRNA (15 nM, QIAGEN) using HiPerFect Transfection Reagent (QIAGEN). After 72 hours, cells were harvested for the detection of DHODH expression.

Quantitative polymerase chain reaction (QPCR)

RNA was extracted using TRIzol reagent (ThermoFisher Scientific, MA, USA) and reverse transcription was performed using PrimeScript RT reagent Kit with gDNA Eraser (Takara, CA, USA). Primers and probes used for QPCR were designed from the Universal ProbeLibrary Assay Design Center (http://www.roche-applied-science.com/). Primers sequence and probes were as follows: DHODH-forward, 5'-AGACTGGCTGTTCGCTTCAC-3'; DHODH-reverse, 5'-TTCCAGCATGTCAGAGTCTTG-3'; DHODH-probe, #45; HIF1A-forward, 5'-AACCTGATGCTTTAACTTTGCTG-3'; HIF1A-reverse, 5'-TGGTCATCAGTTTCTGTGTCG-3'; HIF1A-probe, #28; MMP9-forward, 5'-GAACCAATCTCACCGACAGG-3'; MMP9-reverse, 5'-GCCACCCGAGTGTAACCATA-3'; MMP9-probe, #6; CDH2-forward, 5'-GGTGGAGGAGAAGAAGACCAG-3'; CDH2-reverse, 5'-GGCATCAGGCTCCACAGT-3'; CDH2-probe, #66; Real-time PCR was performed using FastStart Universal Probe Master (Roche Applied Science, Penzberg, Germany) on a LightCycler® 480 (Roche Applied Science). PCR conditions were as follows: 95°C for 10 minutes followed by 45 cycles of 95°C for 15 seconds and 60°C for 1 minute.

Western blot

Cell were lysed by using RIPA buffer with 1% PMSF (Sigma-Aldrich, MO, USA), 1% protease inhibitor (Roche Applied Science) and 1% phosphatase inhibitor (Cell Signaling Technology, MA, USA). The Mini-PROTEAN Tetra Cell (Bio-Rad, CA, USA) system was used for SDS-PAGE electrophoresis. Protein was transferred into Immobilon-P PVDF Membrane (Merck Millipore, CA, USA) by Semi-Dry Electrophoretic Transfer Cell (Bio-Rad). The membrane was incubated for an hour in blocking buffer with gently shaking, followed by incubation with β-tubulin antibodies (Cell Signaling Technology), β-actin antibodies (Cell Signaling Technology), N-cadherin antibodies (Cell Signaling Technology), MMP-9 antibodies (Cell Signaling Technology), DHODH antibodies (Santa Cruz Biotechnology, TX, USA) and HIF1A antibodies (BD Biosciences, CA, USA) overnight at 4°C. After that, the membrane was incubated with secondary antibodies (ThermoFisher Scientific, MA, USA) for an hour at room temperature. Immunoreactivity was detected by WesternBright ECL Spray (advansta, CA, USA). Densitometry analysis of bands was carried out using Image Studio™ Lite (LI-COR Biosciences, NE, USA).

Cell proliferation assay

xCELLigence DP system (ACEA Biosciences Inc., CA, USA) was used for real-time detection of proliferation of oral cancer cell lines. E-Plate 16 (ACEA Biosciences Inc.) was used in proliferation assays. Cells were seeded in E-Plate 16 and cell index of cancer cells was continuously measured.

Colony formation assay

Cells were seeded in a six-well plate with 600 cells in each well. After incubation for 14 days, cells were fixed with 70% ethanol and stained with 0.5% crystal violet. The numbers of colonies with more than 50 cells were counted.

Anoikis analysis

Each well of a 96-well microplate was coated with 10 mg/ml Poly-HEMA (Sigma-Aldrich) and dried overnight in a laminar flow hood at room temperature. OTSCC were seeded into the coated wells. Cell viability was detected by alarmblue cell viability test (ThermoFisher Scientific).

Lentivirus vector construction, lentivirus production, and lentivirus transduction

DHODH-overexpressing lentivector and mock lentivector were custom made from VectorBuilder Inc. (IL, USA). Lentivirus packaging was performed using pPACKH1 HIV Lentivector Packaging Kit (System Biosciences, CA, USA). Lentivirus transduction of CAL27 and SAS cells

was carried out using TransDuxTM MAX Lentivirus Transduction Reagent (System Biosciences).

Cell migration and invasion

xCELLigence DP system (ACEA Biosciences Inc.) was used for real-time detection of migration and invasion of oral cancer cell lines. CIM-Plate 16 (ACEA Biosciences Inc.) was used in migration and invasion assays. For migration assays, the upper chamber was coated with 20 μg/ml fibronectin (Sigma-Aldrich) on both sides. The lower chamber was fulfilled with complete medium. Then, cells were seeded into the upper chamber. For invasion assay, the upper surface of the upper chamber was further coated with Matrigel (BD Biosciences) in 1:50 dilution for 4 hours at 37°C. Cell index of cancer cells was continuously measured.

Flow cytometry analysis

Cells were resuspended in phosphate-buffered saline (PBS) with 2% FBS. Then, cells were stained with antibodies for 10 minutes in the dark at 2-8°C. For intracellular proteins, cells were fixed with 2% paraformaldehyde and permeabilization buffer containing 0.5% Tween-20 followed by incubation with antibodies. After washing twice with PBS, cells were resuspended into 300 μL of PBS and fluorescence was measured by using CytoFLEX S flow cytometer (Beckman Coulter, Inc., IN, USA).

Xenograft model and pulmonary metastasis animal model

All animal experiments were performed according to the institutional guidelines and were approved by the Institutional Committee on the Use of Live Animals in Teaching and Research (protocol no. 4606-18) at the Animal Laboratory, Department of Surgery, University of Hong Kong (Hong Kong, SAR, China). For xenograft model, DHODH-overexpressing SAS (1×10^6 cells in 100 μl) or control SAS (1×10^6 cells in 100 μl) were injected subcutaneously into the flank of athymic nu/nu mice (5 weeks old, weight range: 18-22 g). The tumor size was measured daily in two dimensions using calipers and the tumor volume was calculated using the following formula: Volume (mm^3) = $(L\times W^2)/2$, where L is the length (mm) and W is the width (mm). At the end of the experiment, all mice were sacrificed and the tumors were harvested. For pulmonary metastasis animal model, oral cancer cells were injected into nude mice via tail vein. DHODH-overexpressing SAS (7.5×10^5) or control SAS (7.5×10^5) were suspended in 250 μl PBS containing 0.1% BSA to avoid cell gathering. Following circulation system, injected cells migrated and gathered in lung, and developed metastatic foci. The body weight of nude mice was measured twice a week. The nude mice were sacrificed after 45 days and their lung tissue samples were collected. The number of metastatic foci was then counted. H&E staining was performed on lung section.

H_2O_2, antioxidant and DHODH inhibitor treatment

H_2O_2 (Sigma-Aldrich), N-Acetyl-L-cysteine (NAC, Sigma-Aldrich) and ammonium pyrrolidinedithiocarbamate (PDTC, Sigma-Aldrich) were used to treat OTSCC cells for 72 h, 8 h and 24 h, respectively. Two DHODH inhibitors, leflunominde (ABCAM) and atovaquone (Sigma-Aldrich), were used to treat OTSCC cells for 72 h.

ROS detection

Dichloro-dihydro-fluorescein diacetate (DCFH-DA, Sigma-Aldrich) was used to detect ROS on a flow cytometer. Cells were stained with 10 μM DCFH-DA at 37°C for 15 minutes. Intracellular DCFH-DA could be oxidized into DCF with fluorescence by cellular ROS. Fluorescence signal was measured by using CytoFLEX S (Beckman Coulter, CA, USA) and data was analysed by FlowJo 7.6 (FlowJo LLC, OR, USA).

Hypoxia treatment

Incubator chamber (billups-rothenberg, CA, USA) fulfilled with low-oxygen gas (Linde, Dublin, Ireland) containing 1% O_2, 5% CO_2 and 94% N_2 was used to build hypoxic environment. The hypoxic chamber was incubated in humidified incubator at 37°C.

Transcription activation activity of HIF-1 protein

HIF-1-responsive luciferase construct was obtained from Addgene (HRE-luciferase, plas-

mid #26731). HRE-luciferase vector contained three hypoxia response elements (HRE, TGTCACGTCCTGCACGACTCTAGT). HRE-luciferase vector was transfected into OTSCC cells using Lipofectamine 3000 Transfection Reagent (ThermoFisher Scientific). Dual-Luciferase assay (Promega, WI, USA) was performed to measure the changes in HIF-1 activity.

Immunohistochemistry (IHC)

Formalin-fixed, paraffin-embedded mouse xenograft was cut into 4 μm sections. IHC was performed to measure the expression of DHODH and HIF1A. After antigen retrieval and peroxidase blocking, sections were incubated with HIF1A antibodies (ABCAM, Cambridge, UK) and DHODH antibodies (BD Biosciences). IHC visualization was performed using REAL EnVDetectSys Perox/DAB+ (DAKO, CA, USA).

Statistical analysis

All results were shown as averages and presented as mean ± SD from three or more independent experiments. Data were processed and analyzed with Excel (Microsoft, WA, USA) or SPSS V20.0 (Armonk, NY, USA). All the tests were 2-sided. *P*-values <0.05 were considered as statistical significance.

Results

Increased DHODH expression was associated with clinicopathological features of head and neck cancer patients

To investigate the clinical significance of DHODH expression in head and neck cancer, we evaluated the association of DHODH level with the clinical parameters of head and neck cancer patients in The Cancer Genome Atlas (TCGA). DHODH mRNA level was significantly increased in tumor tissues in comparison with normal tissues (**Figure 1A**). High DHODH was significantly associated with advanced tumor stage (**Figure 1B**). Poorly and moderately differentiated tumors showed a higher expression of DHODH than well-differentiated ones (**Figure 1C**). These results indicated that high DHODH expression might be involved in tumorigenesis and aggressive phenotype in head and neck cancer. High DHODH level was found in the males as compared with the female patients (**Figure 1E**). DHODH level did not show a significant difference between HPV-positive patients and negative ones (**Figure 1D**).

Aberrant DHODH methylation in head and neck cancers

Eleven probes were used to examine the methylation status of CpGs of the DHDOH gene in TCGA. Among the 11 probes, 10 probes are located at the promoter region of DHODH (from 1267 bp upstream of TSS to 282 bp downstream of TSS) (**Figure 2A**). The probe cg16579770 is located at the transcript coding region (at -16295 to TSS). Among the ten probes situated in the promoter region, cg22381196, cg19061957, cg10190104, cg00157456, cg06220725, and cg07817698 showed significant difference in methylation level between tumor and normal tissue (**Figure 2B**). Aggregation box plot was used to indicate the mean methylation of all the ten probes. Results revealed that DHODH promoter methylation was significantly reduced in head and neck cancer tissues as compared to normal tissues (**Figure 2B**, **2C**). Methylation of CpGs mapped by cg16579770 was significantly increased in the tumor as compared to normal tissue (**Figure 2D**). Moreover, the methylation level of cg16579770 was significantly associated with the stage of head and neck cancers (**Figure 2E**).

DHODH modulated OTSCC proliferation and colony formation

To address whether DHODH has a functional role in oral cancers, we knockdown DHODH using two different siRNAs (**Figure 3A**, **3B**) and examined cell proliferation using real-time cell proliferation assays. OTSCC proliferation was significantly reduced after knockdown of DHODH (**Figure 3C**). Further, knockdown DHODH increased the doubling time (**Figure 3D**) and inhibited colony formation ability of OTSCC cells (**Figure 3E**, **3F**).

DHODH enhanced anoikis resistance, migration, and invasion of OTSCC

We addressed whether DHODH promoted anchorage-independent growth (resistance to anoikis) and increased invasiveness [20]. First, OTSCC were seeded in culture plates coated with poly-HEMA, and the cell viability was measured using alamarBlue assay. Knockdown

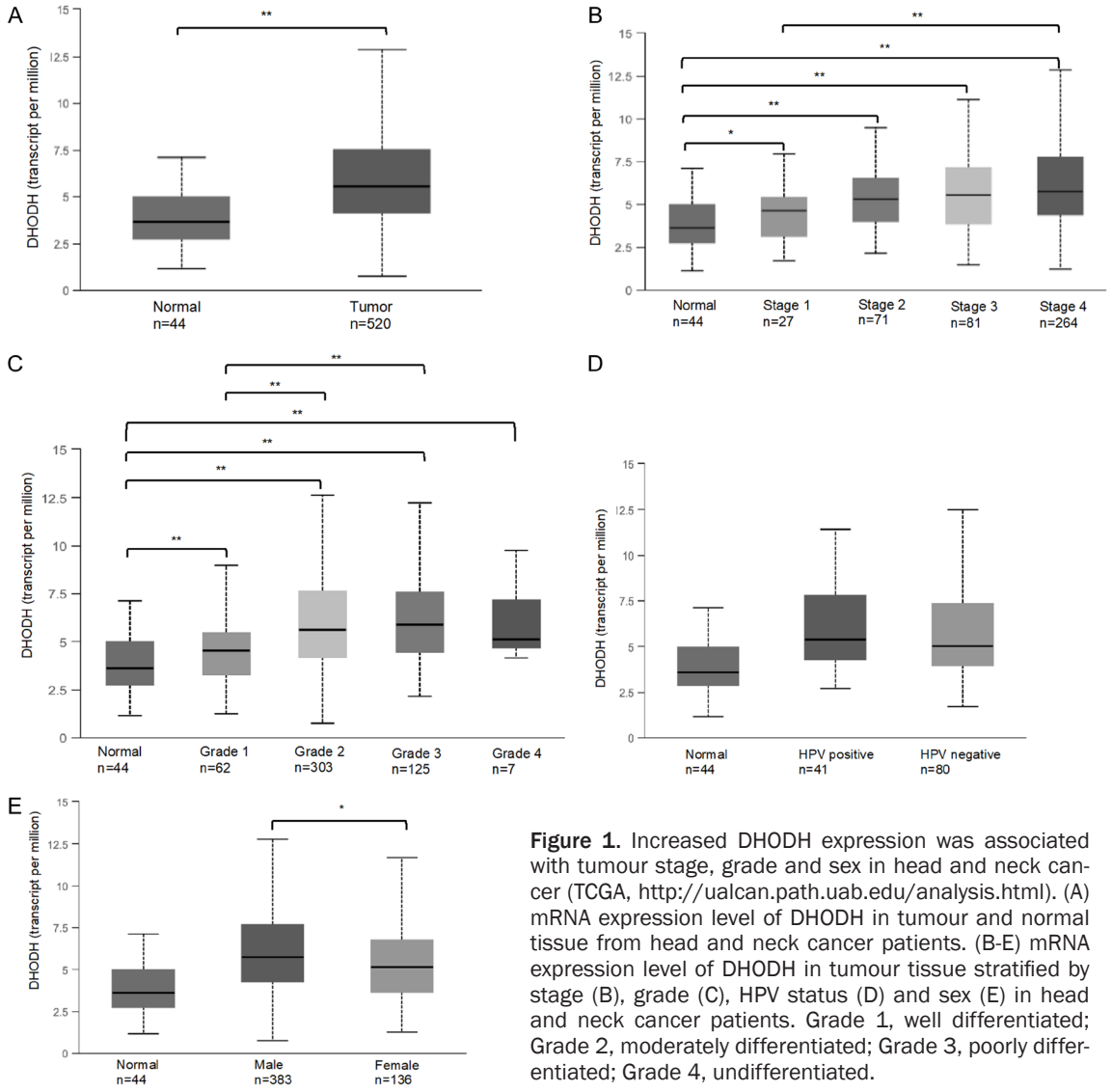

Figure 1. Increased DHODH expression was associated with tumour stage, grade and sex in head and neck cancer (TCGA, http://ualcan.path.uab.edu/analysis.html). (A) mRNA expression level of DHODH in tumour and normal tissue from head and neck cancer patients. (B-E) mRNA expression level of DHODH in tumour tissue stratified by stage (B), grade (C), HPV status (D) and sex (E) in head and neck cancer patients. Grade 1, well differentiated; Grade 2, moderately differentiated; Grade 3, poorly differentiated; Grade 4, undifferentiated.

DHODH significantly reduced cell viability under anchorage-independent growth conditions (**Figure 4A**). To confirm the data, we repeated the cell viability assay in DHODH-overexpressing lines (**Figure 4B**). Increased DHODH expression led to a significant increase in cell viability under anchorage-independent growth conditions (**Figure 4C**). The results indicate that DHODH promoted anoikis resistance in OTSCC. Then, we examined the changes in migration/invasion ability of DHODH-knockdown and -overexpressing OTSCC cells using the xCELLigence DP system. DHODH knockdown significantly inhibited migration and invasion (**Figure 4D**), while DHODH overexpression enhanced migration and invasion (**Figure 4E**). Further, results from flow cytometry analysis showed that DHODH overexpression increased the protein expression level of epithelial-mesenchymal transition (EMT) markers CDH2, MMP9 and ZEB2 in oral cancer cells (**Figure 4F**). In contrast, DHODH overexpression decreased the expression of CDH1 (**Figure 4F**). To investigate whether DHODH regulated EMT markers via HIF1A, DHODH-overexpressing cells were transfected with HIF1A siRNA and the expression of EMT markers were determined again. Silencing of HIF1A abrogated the increase of CDH2, MMP9 and ZEB2 expression induced by DHODH overexpression (**Figure 4F**), implicating that DHODH modulated EMT markers at least partially through HIF1A.

A

Probe	Chromosome	Start	End	CGIposition	Strand	Distance_To_TSS
cg22381196	chr16	72007477	72007478	N_Shore	+	1267
cg19061957	chr16	72008449	72008450	Island	+	295
cg10190104	chr16	72008451	72008452	Island	+	293
cg00157456	chr16	72008473	72008474	Island	-	271
cg08830573	chr16	72008583	72008584	Island	-	161
cg06220725	chr16	72008692	72008693	Island	+	52
cg01557791	chr16	72008794	72008795	Island	+	-50
cg14768367	chr16	72008959	72008960	Island	+	-215
cg00580805	chr16	72008988	72008989	Island	+	-244
cg07817698	chr16	72009026	72009027	S_Shore	+	-282
cg16579770	chr16	72025039	72025040		+	-16295

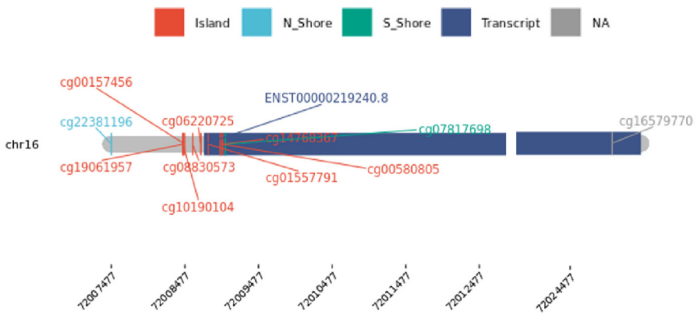

B

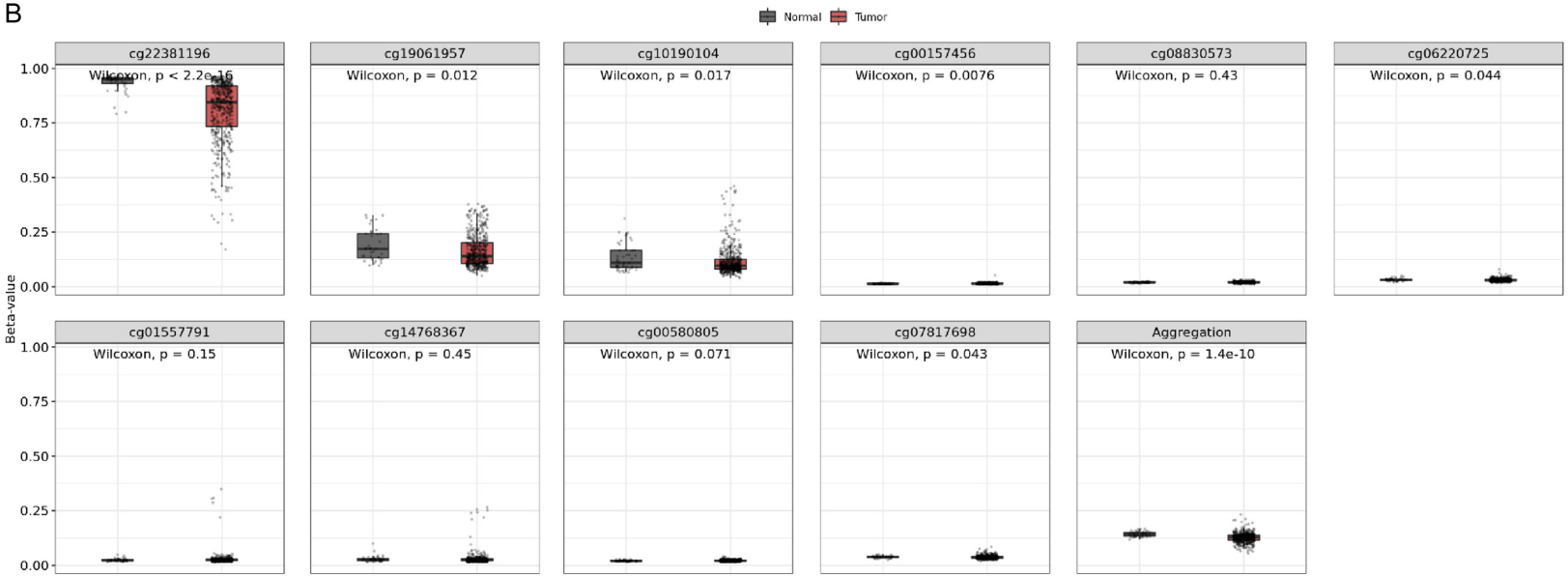

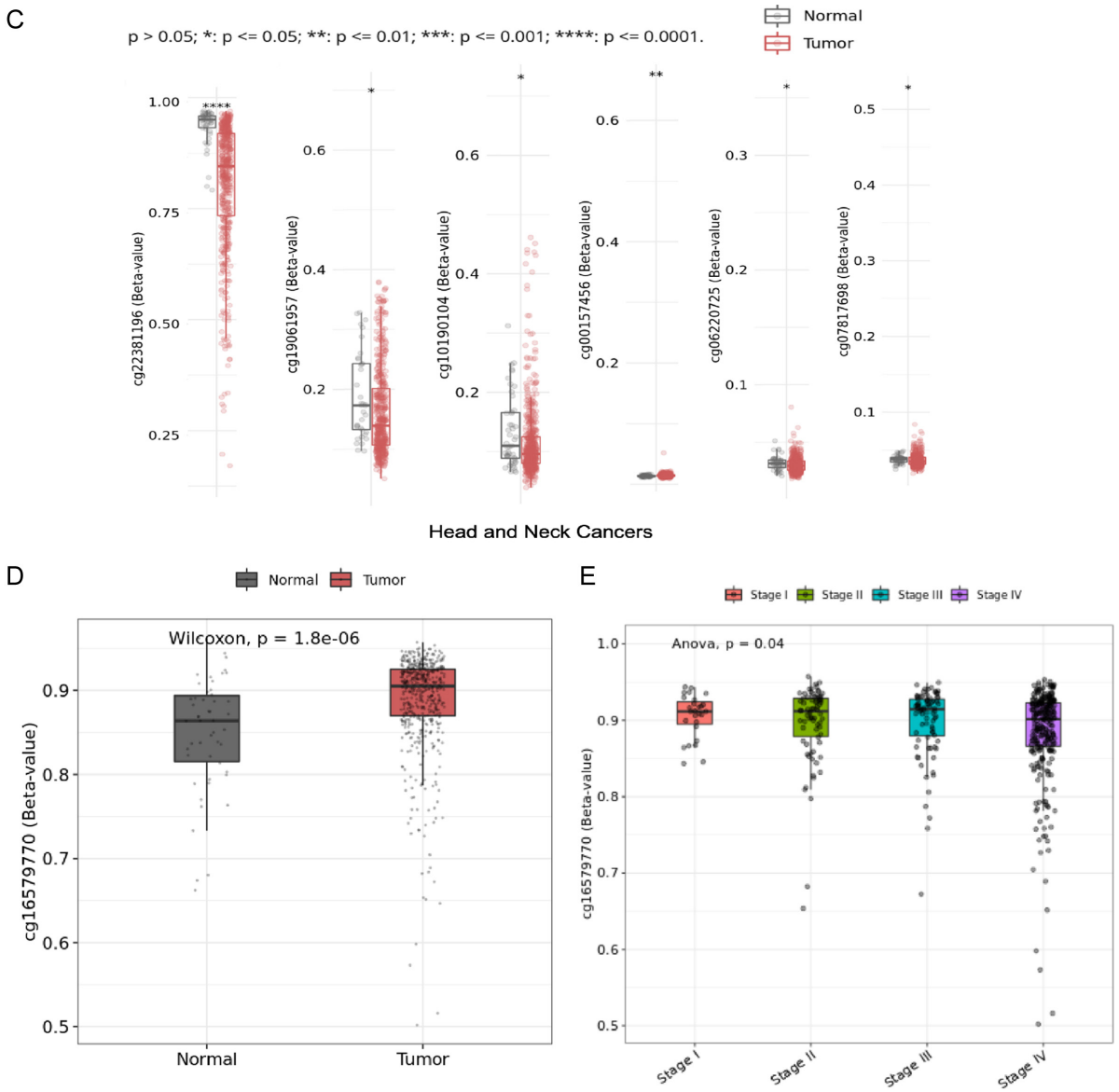

Figure 2. DHODH promoter was hypomethylated in tumour of head and neck cancer patients (TCGA, http://www.bioinfo-zs.com/smartapp/). A. Location of 11 probes. B and C. Methylation levels of 10 probes in promoter region of DHODH in head and neck cancer patients. D. Methylation level of probe cg16579770 in head and neck cancer patients. E. Methylation level of cg16579770 in tumour tissue stratified by stage in head and neck cancer patients.

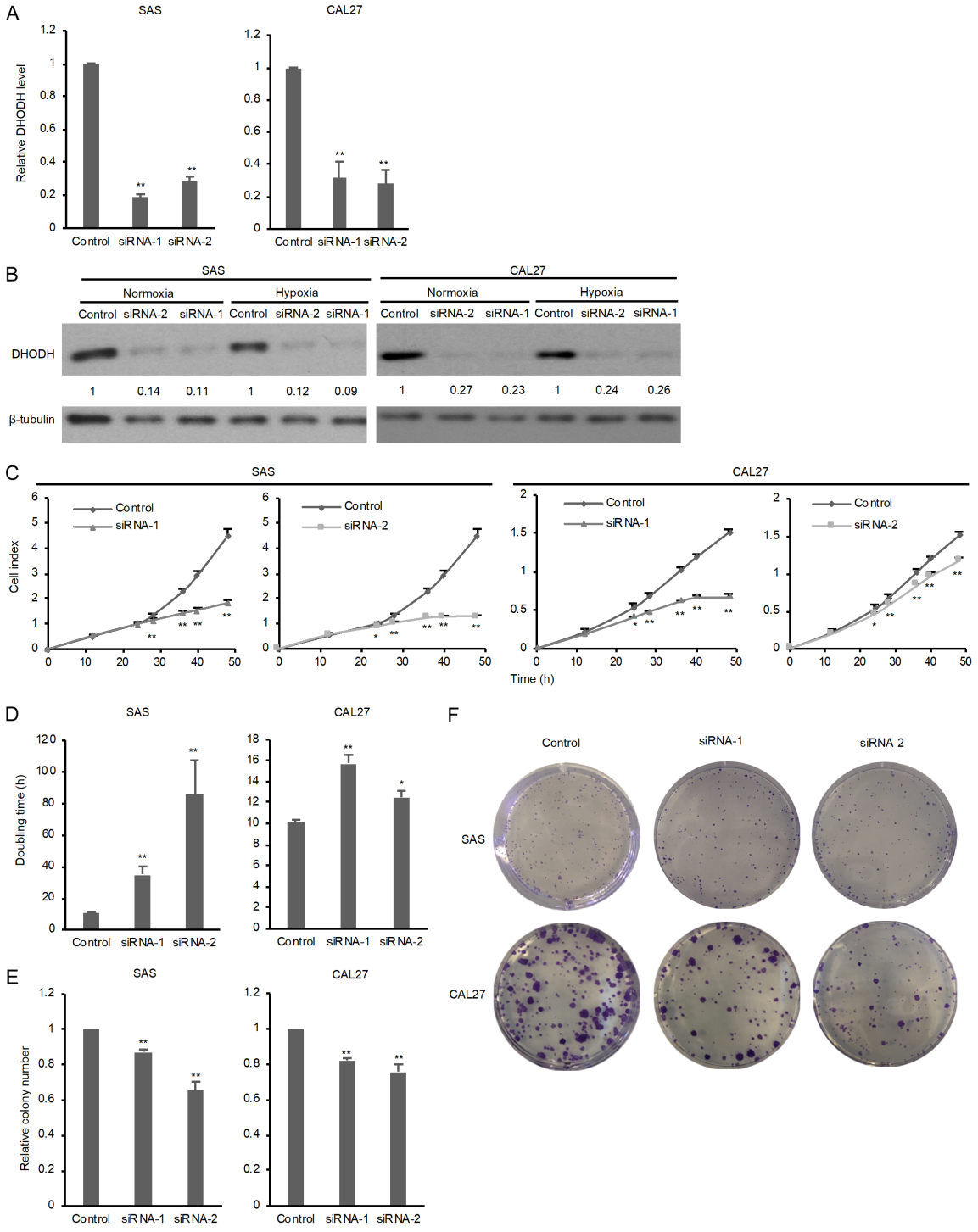

Figure 3. DHODH enhanced proliferation and colony formation of OTSCC. (A) QPCR analysis of DHODH expression in OTSCC cells transfected with DHODH-siRNA-1 (15 nM) or DHODH-siRNA-2 (15 nM) or negative control siRNA (15 nM). (B) Western blot analysis of DHODH expression in OTSCC cells transfected with DHODH siRNA or negative control siRNA. β-tubulin was used as loading control. Densitometry analysis of bands was carried out using Image Studio™ Lite. Densitometry values of DHODH were normalized to β-tubulin and displayed under each blot. (C, D) Cell proliferation (C) and doubling time (D) of OTSCC cells transfected with DHODH siRNA or negative control siRNA using xCELLigence DP system. (E) Colony formation assay of OTSCC cells transfected with DHODH siRNA or negative control siRNA. (F) Representative images of colony formation in (E). Data are expressed as mean ± SD (n=3). *P<0.05, **P<0.01 (Student t test).

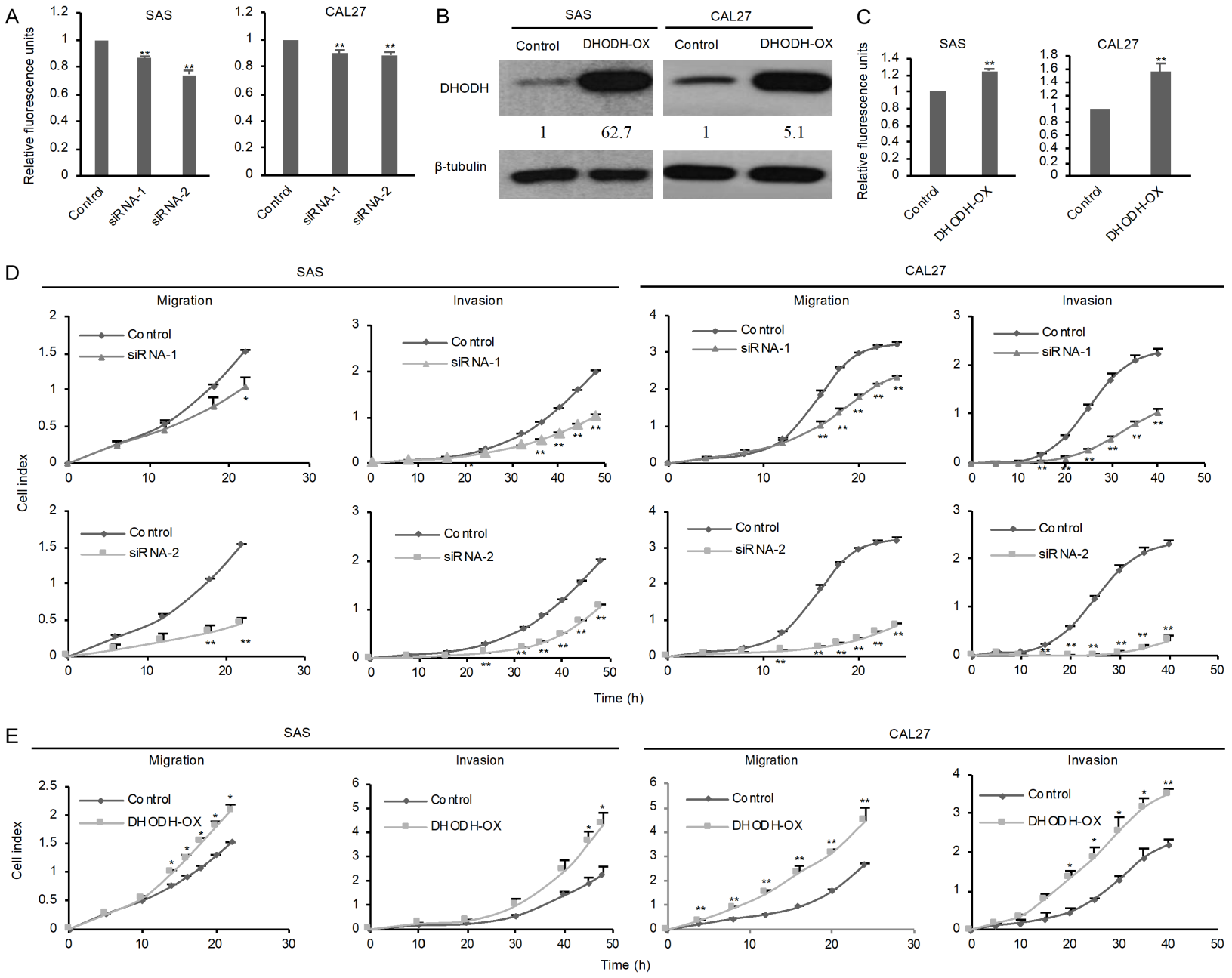
A
SAS
CAL27
Relative fluorescence units
Control
siRNA-1
siRNA-2
B
SAS
CAL27
Control
DHODH-OX
DHODH
β-tubulin
1
62.7
1
5.1
C
SAS
CAL27
Relative fluorescence units
Control
DHODH-OX
D
SAS
CAL27
Migration
Invasion
Cell index
Time (h)
E
SAS
CAL27
Migration
Invasion
Cell index
Time (h)

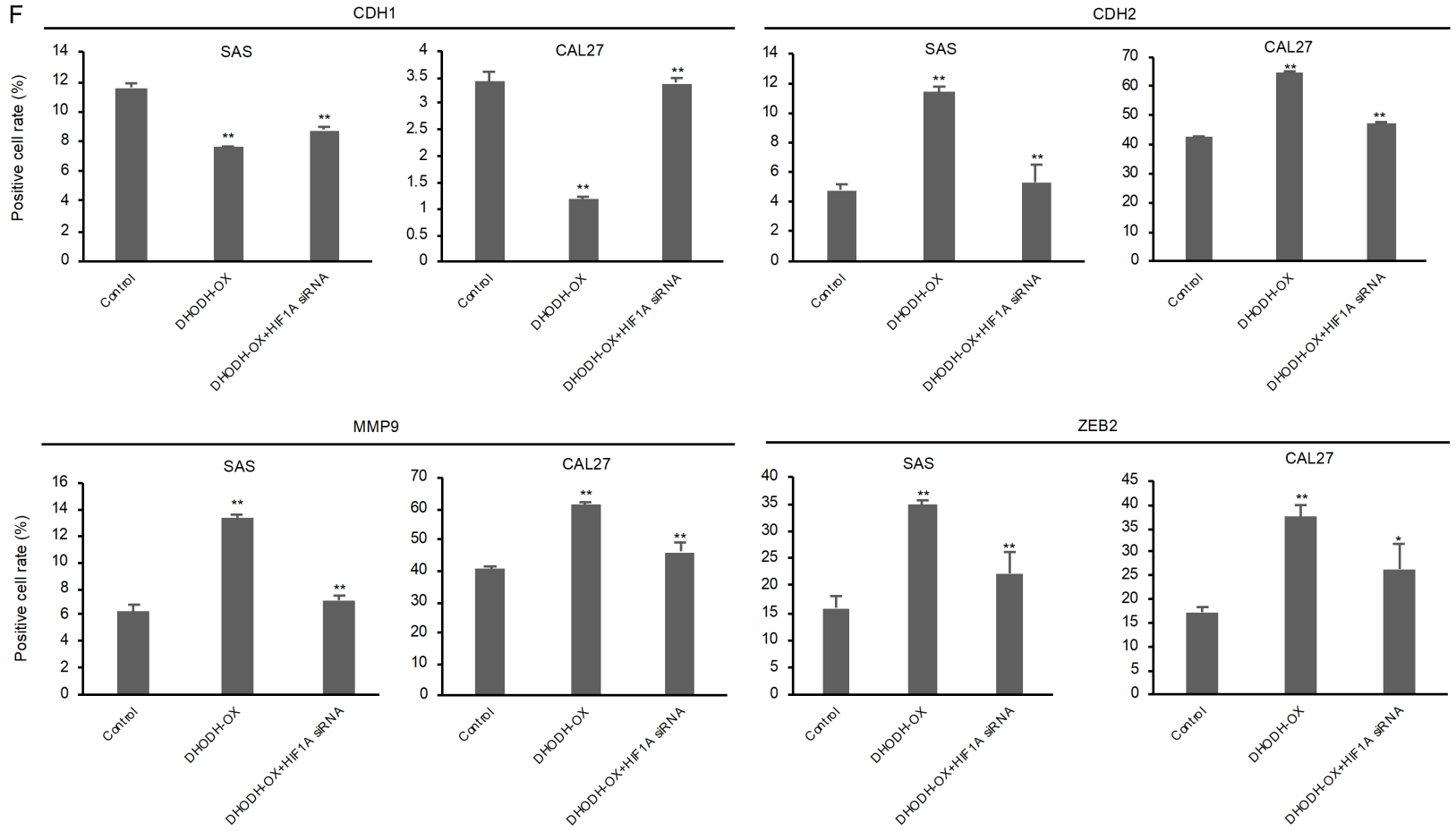

Figure 4. DHODH promoted migration and invasion in OTSCC. (A) Analysis of anoikis in OTSCC cells transfected with DHODH-siRNA-1 (15 nM) or DHODH-siRNA-2 (15 nM) or negative control siRNA (15 nM). (B) Western blot analysis of DHODH expression in DHODH-overexpressing OTSCC cells. Densitometry values of DHODH were normalized to β-tubulin and displayed under each blot. (C) Analysis of anoikis in DHODH-overexpressing OTSCC cells. (D, E) Real-time monitor of cell migration and invasion using xCELLigence DP system in OTSCC cells transfected with DHODH siRNA (D) and DHODH-overexpressing OTSCC cells (E). (F) Flow cytometry analysis of expression levels of EMT-related genes in DHODH-overexpressing OTSCC cells. Data are expressed as mean ± SD (n=3). $^{*}P<0.05$, $^{**}P<0.01$ (Student t test).

DHODH prompted tumor growth and metastasis in vivo

Given that DHODH increased OTSCC proliferation and invasion *in vitro*, we validated the findings using *in vivo* xenograft model. DHODH-overexpressing SAS cells and control cells were subcutaneously injected into nude mice to generate xenograft tumors. DHODH overexpression promoted tumor growth over time (**Figure 5A**, **5B**). The final tumor weight was also increased in xenograft derived from DHODH-overexpressing cells (**Figure 5C**). Also, we tested whether DHODH increased metastasis *in vivo* using pulmonary metastasis animal model. DHODH-overexpressing SAS cells and control cells were inoculated into nude mice via tail vein and metastatic foci in the lung were measured. Thirty-seven days after tumor cell inoculation, body weight began to decrease in a mouse injected with DHODH-overexpressing SAS cells (**Figure 5E**). A higher number of lung metastatic foci was observed in mice inoculated with DHODH-overexpressing SAS cells (**Figure 5D**, **5F**). H&E staining showed that more and larger lung metastatic foci were observed in the DHODH-overexpressing group as compared with the control group (**Figure 5G**).

HIF1A expression was controlled by reactive oxygen species (ROS) in OTSCC

To test the role of ROS in activating HIF1A expression, we treated OTSCC cells with H_2O_2 or two different ROS scavengers (NAC and PDTC). H_2O_2 treatment increased the mRNA level of HIF1A in a dose-dependent manner (**Figure 6A**). In contrast, NAC and PDTC treatment resulted in a dose-dependently suppression of HIF1A mRNA in OTSCC (**Figure 6B**, **6C**). The results suggested that OTSCC ROS has a stimulating effect on HIF1A transcription.

DHODH governed HIF1A expression by ROS

DHODH is a ROS-generating enzyme in OTSCC. Knockdown of DHODH significantly decreased intracellular ROS production (**Figure 7A**). Knockdown of DHODH significantly inhibited HIF1A mRNA (**Figure 7B**) and protein (**Figure 7C**) level under both normoxic and hypoxic conditions. The results suggested that DHODH has a regulatory function on HIF1A expression in OTSCC. Next, we asked whether DHODH overexpression altered the HIF-1 activity in OTSCC. After translocation to the nucleus, dimeric HIF-1 binds to the hypoxia-response element (HRE) of its target genes and activates gene transcription [21]. To measure the transcription activation activity of HIF-1, OTSCC were transfected with HIF1-responsive luciferase construct (HRE-luciferase) and 2 DHODH-specific siRNAs. HRE-luciferase vector contained luciferase gene under the control of three HRE. Therefore luciferase activity reflected the transcription activation activity of HIF-1. Knockdown of DHODH suppressed the transcription activation activity of HIF-1 under both normoxic and hypoxic conditions (**Figure 7D**). To answer whether DHODH controls HIF1A expression via the ROS-generating function, DHODH-overexpressing cells were treated with NAC and expression level of HIF1A was determined by QPCR and western blot. NAC treatment inhibited mRNA and protein levels of HIF1A in DHODH-overexpressing OTSCC (**Figure 7E**, **7F**), implicating that DHODH enhanced HIF1A expression via ROS production. Moreover, NAC treatment inhibited the transcription activation activity of HIF-1 in DHODH-overexpressing cells (**Figure 7G**). To test whether DHODH increased the protein stability of HIF1A, we treated CAL27 cells with cycloheximide (CHX) to inhibit de novo protein synthesis and evaluated the protein level of HIF1A at 15, 30 and 45 minutes. Knockdown of DHODH using siRNA decreased the stability of HIF1A protein (**Figure 7H**). To validate the regulatory role of DHODH on HIF1A expression in vivo, the expression of DHODH and HIF1A were measured in xenografts derived from DHODH-overexpressing SAS cells and control cells using IHC. A higher expression of both DHODH and HIF1A was observed in xenografts derived from DHODH-overexpressing SAS cells in comparison with control cells (**Figure 7I**), indicating that DHODH promoted HIF1A expression *in vivo*. Moreover, more cells showed accumulation of HIF1A protein in the nucleus in DHODH-overexpressing SAS cells as compared to control cells (**Figure 7I**).

Pharmacological DHODH inhibitor suppresses HIF1 activity in OTSCC

To test whether targeting DHODH is potentially useful in OTSCC treatment, 2 FDA-approved DHODH inhibitors (leflunomide and atovaquone) were tested. Both leflunomide and atovaquone can reduce ROS production in OTSCC

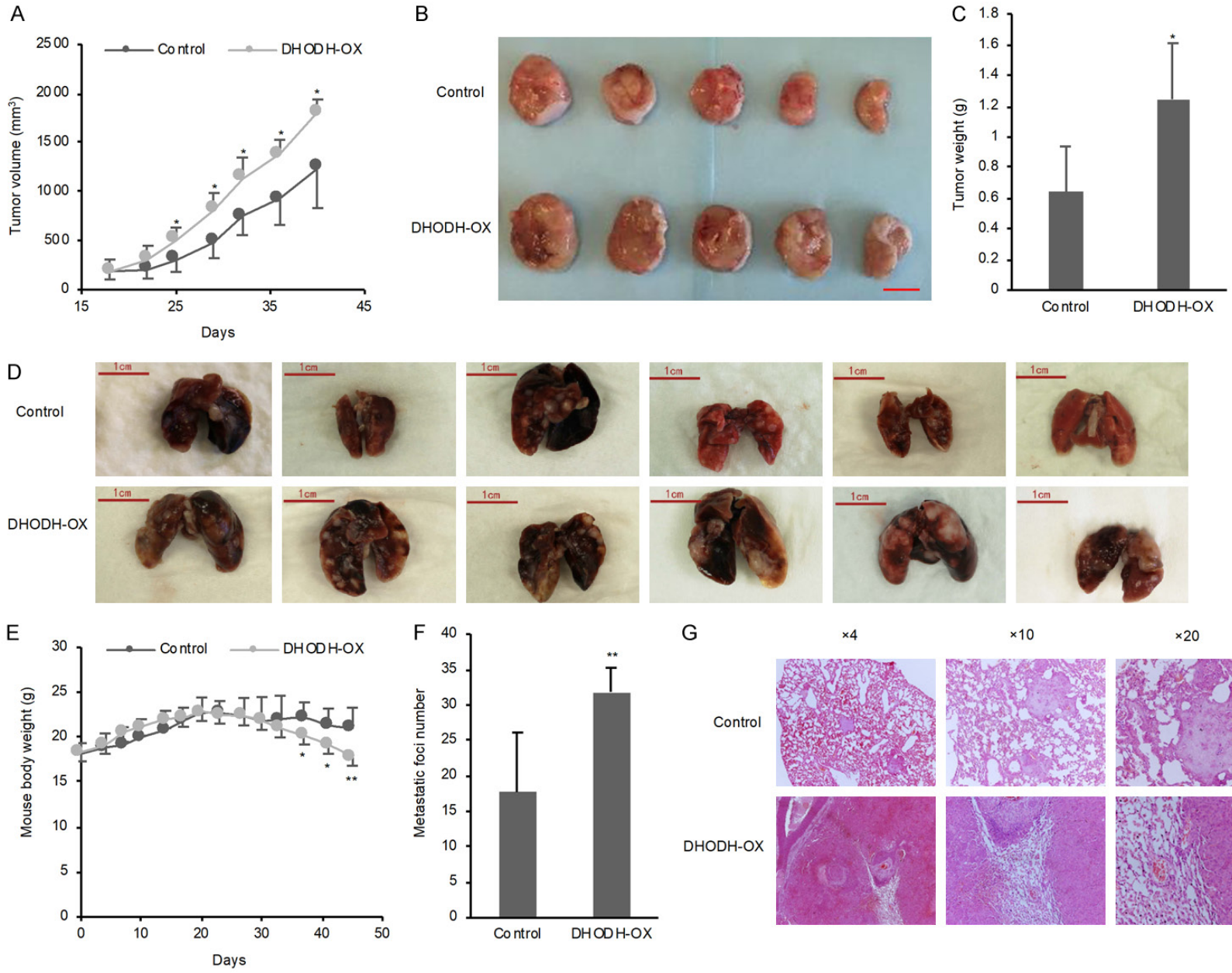
A
Control
DHODH-OX
Tumor volume (mm³)
Days
B
Control
DHODH-OX
C
Tumor weight (g)
Control
DHODH-OX
D
Control
DHODH-OX
1cm
E
Control
DHODH-OX
Mouse body weight (g)
Days
F
Metastatic foci number
Control
DHODH-OX
G
×4
×10
×20
Control
DHODH-OX

Figure 5. DHODH enhanced tumor growth and metastasis in OTSCC. (A-C) Xenograft model. Tumor volume over time (A) and final tumor weight (C) of xenografts derived from DHODH-overexpressing SAS cells and control cells. Images of excised tumor were shown in (B). (D-G) Metastasis model. (D) Images of lungs from mice injected with DHODH-overexpressing SAS cells and control cells. (E) Body weight of mice. (F) The number of metastasis foci on the lung. (G) Representative images of H&E-stained lungs from mice injected with DHODH-overexpressing SAS cells and control cells. Data are expressed as mean ± SD (n=5 for A, C; n=6 for E, F). *P<0.05, **P<0.01 (Student t test).

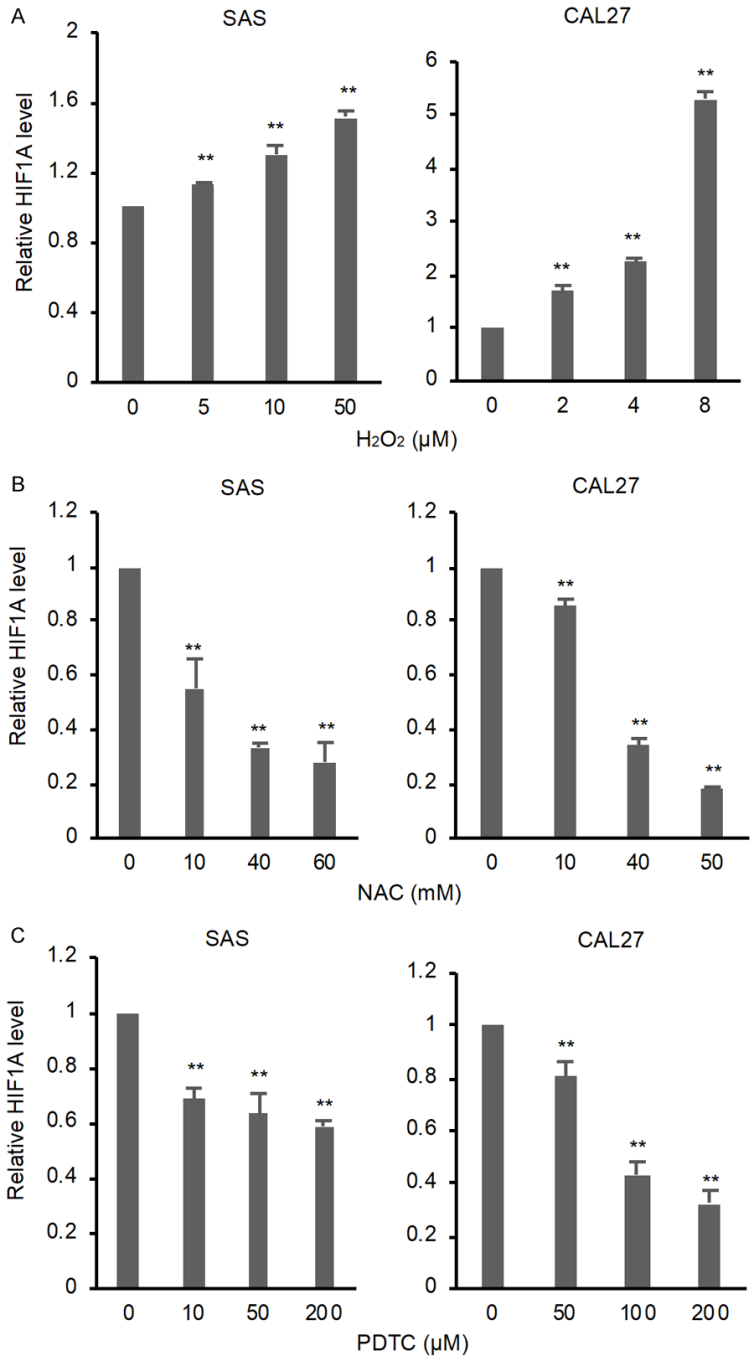

Figure 6. ROS enhanced HIF1A expression in OTSCC. QPCR analysis of HIF1A expression in OTSCC cell treated by H2O2 (A), NAC (B) and PDTC (C). Data are expressed as mean ± SD (n=3). **P<0.01 (One-way analysis of variance followed by a Tukey's test).

cells (**Figure 8A**). Leflunomide and atovaquone treatment suppressed HIF1A mRNA and protein expression in both normoxic and hypoxic conditions (**Figure 8B**, **8C**). Atovaquone treatment inhibited the transcription activation activity of HIF-1 (**Figure 8D**). In contrast, leflunomide did not alter the transcription activation activity of HIF-1 (**Figure 8D**). Functionally, atovaquone treatment significantly suppressed proliferation (**Figure 8E**), colony formation (**Figure 8F**), and migration/invasion (**Figure 8G**) of OTSCC cells. These results suggested that targeted treatment with atovaquone might potentially be useful in OTSCC treatment.

Discussion

In the current study, we found that head and neck cancers have high expression of DHODH. Besides, a high DHODH level is significantly associated with the clinicopathological features of head and neck cancer patients. Reduced CpG island methylation in the promoter region is one of the possible causes related to the high DHODH level in head and neck cancer cells. Of the 11 CpGs examined, we noticed that methylation of CpG on the coding region of DHODH (-16295) is remarkably increased in head and neck cancers as compared with the normal controls. Generally, CpG methylation at the promoter region will inhibit transcription initiation result-

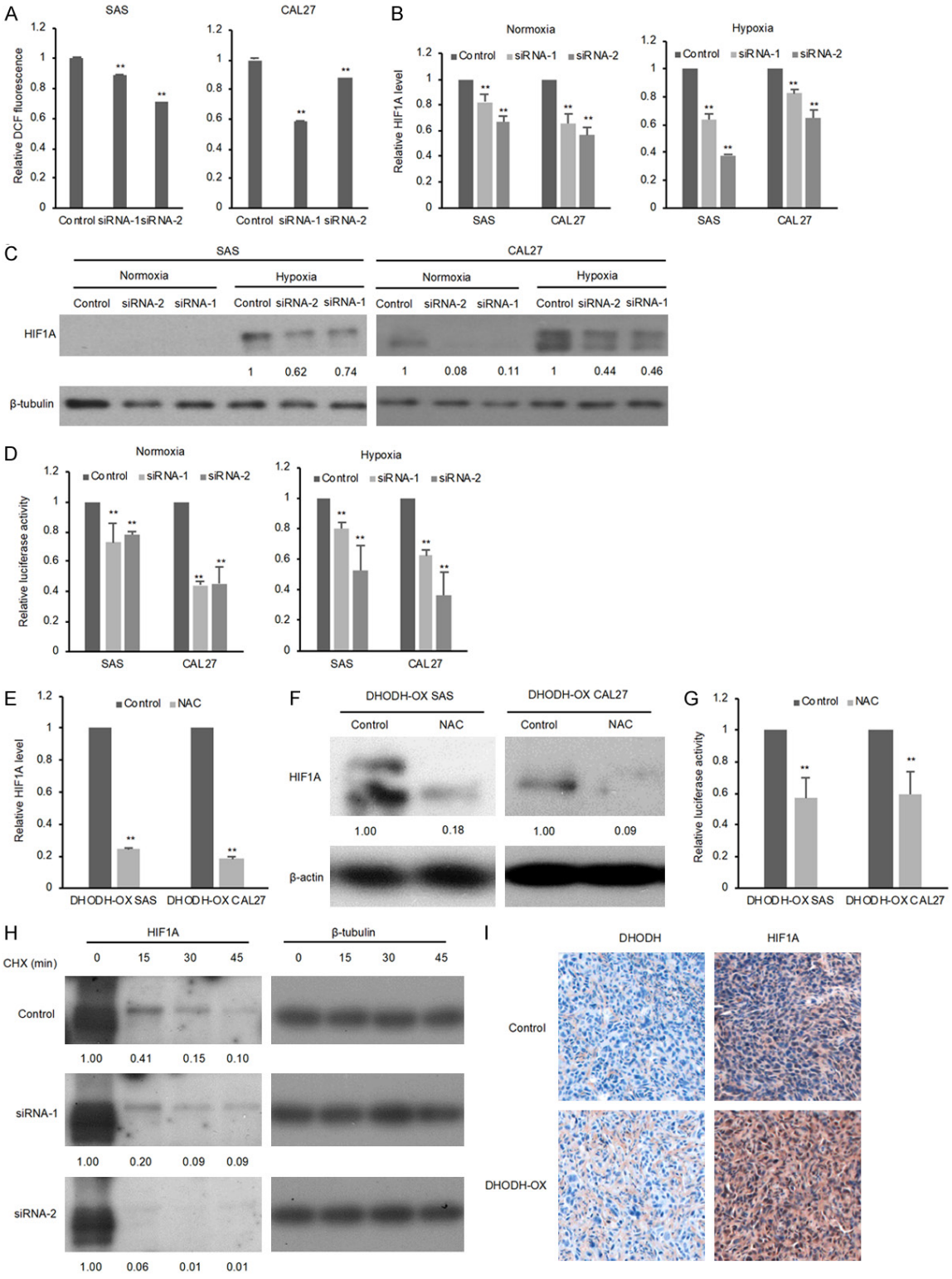

Figure 7. DHODH promoted HIF1A expression via ROS. A. Flow cytometry analysis of ROS production in OTSCC cells transfected with DHODH siRNA or negative control siRNA. B. QPCR analysis of HIF1A expression in OTSCC cells transfected with DHODH siRNA or negative control siRNA. C. Western blot analysis of HIF1A expression in OTSCC cells transfected with DHODH siRNA or negative control siRNA. β-tubulin was used as loading control. Densitometry analysis of bands was carried out using Image Studio™ Lite. Densitometry values of HIF1A were normalized to β-tubulin and displayed under each blot. D. Dual luciferase analysis of transcription activation activity of HIF-1

in OTSCC cells transfected with DHODH siRNA or negative control siRNA. E. QPCR analysis of HIF1A expression in DHODH-overexpressing OTSCC cells treated by NAC (10 mM). F. Western blot analysis of HIF1A expression in DHODH-overexpressing OTSCC cells treated by NAC (10 mM). G. Dual luciferase analysis of transcription activation activity of HIF-1 in DHODH-overexpressing OTSCC cells treated by NAC (10 mM). H. Western blot analysis of HIF1A expression in CAL27 cells treated with CHX (100 μg/ml). I. IHC analysis of DHODH and HIF1A expression in xenograft derived from DHODH-overexpressing SAS cells and control cells. Data are expressed as mean ± SD (n=3). $^{**}P<0.01$ (Student t test).

ing in epigenetic silencing of the associated genes. The functional implication of CpG methylation on the gene coding region and transcription is less clear. In plant protoplasts, it has been reported that CpG methylation of the coding region still has a negative impact on expression in gene without methylation sites in the promoter regulatory region [22].

DHODH is a ROS-generating enzyme in oral cancers with key functional implication. DHODH increases proliferation and colony formation ability. DHODH overexpression promotes oral cancer growth and development in the pre-clinical model. Also, oral cancers with high DHODH expression are more aggressive with a higher capacity to migrate and invade. Our findings provide evidence suggesting that DHDOH promotes tumorigenesis of oral cancers. DHODH catalyzes the ubiquinone-mediated oxidation of dihydroorotate to orotate in the de novo pyrimidine biosynthesis process and ATP synthesis. Thus, it is speculated that DHODH is playing an active role in oral cancer proliferation. It is believed that DHODH is essential for the initial phases of the carcinogenesis of epithelial cancers [23]. Our results provide evidence suggesting that DHODH could also increase the invasiveness of cancers, but the mechanism of action remains poorly understood.

Mitochondria can coordinate signal cascade responsible for the hypoxic transcription activity mediated by HIF-1. Several studies have shown that inhibiting the enzymes involved in the oxidative phosphorylation process of mitochondria will destabilize HIF-1 under hypoxic conditions. Inhibition of mitochondrial complex I, the first enzyme in the mitochondrial electron transport chain of mitochondria, can reduce oxygen consumption and inhibit the hypoxia-induced accumulation of HIF1A in human hepatoma cells [24]. It has been reported that ROS-generating enzyme can stimulate HIF1A transcription in cancer cells. Therefore, we speculated that DHODH might function as a transcription activator of HIF1A in oral cancers.

Increased ROS has a positive impact on HIF-1A accumulation. ROS could inhibit PHD activity, thus enhanced the stability of HIF1A [25, 26]. Using H_2O_2 as an external source of ROS, we noticed that HIF1A mRNA was significantly increased in OTSCC. As DHODH promote ROS generation in OTSCC, we addressed whether DHODH modulated HIF1A expression. As expected, DHODH promoted transcription, protein stability, and transactivation activity of HIF1A. Additionally, DHODH induced HIF1A upregulation in OTSCC can be reversed with the use of ROS scavenger. Again, the data highlighted that DHODH could exert gene and signal regulatory function via ROS.

Given that targeting DHODH with specific siRNA inhibits oral cancer proliferation, migration, and invasion. We speculate that the DHODH inhibitor, which is readily available clinically are useful for oral cancer treatment. Therefore, we evaluate the effectiveness of leflunomide and atovaquone which function differently in oral cancer cell lines. Leflunomide is an FDA-approved drug for rheumatoid arthritis [27]. The metabolite of leflunomide, A77 1726, could reversibly inhibit DHODH activity by competing with the substrates ubiquinone competitively and dihydroorotate noncompetitively [28]. Atovaquone is an FDA-approved drug for malaria [29]. Atovaquone was safe and well-tolerated in humans [30]. Atovaquone is a direct non-competitive inhibitor of dihydroorotate binding site on DHODH [31]. Atovaquone could also inhibit complex III and prevent the formation of ubiquinone, the substrate of DHODH [29]. Our data showed that both leflunomide and atovaquone could reduce ROS level and HIF1A expression in OTSCC. However, reduced overall HIF-1 activity is only observed in OTSCC treated with atovaquone.

In conclusion, our results suggested that DHODH promotes oral cancer by increasing

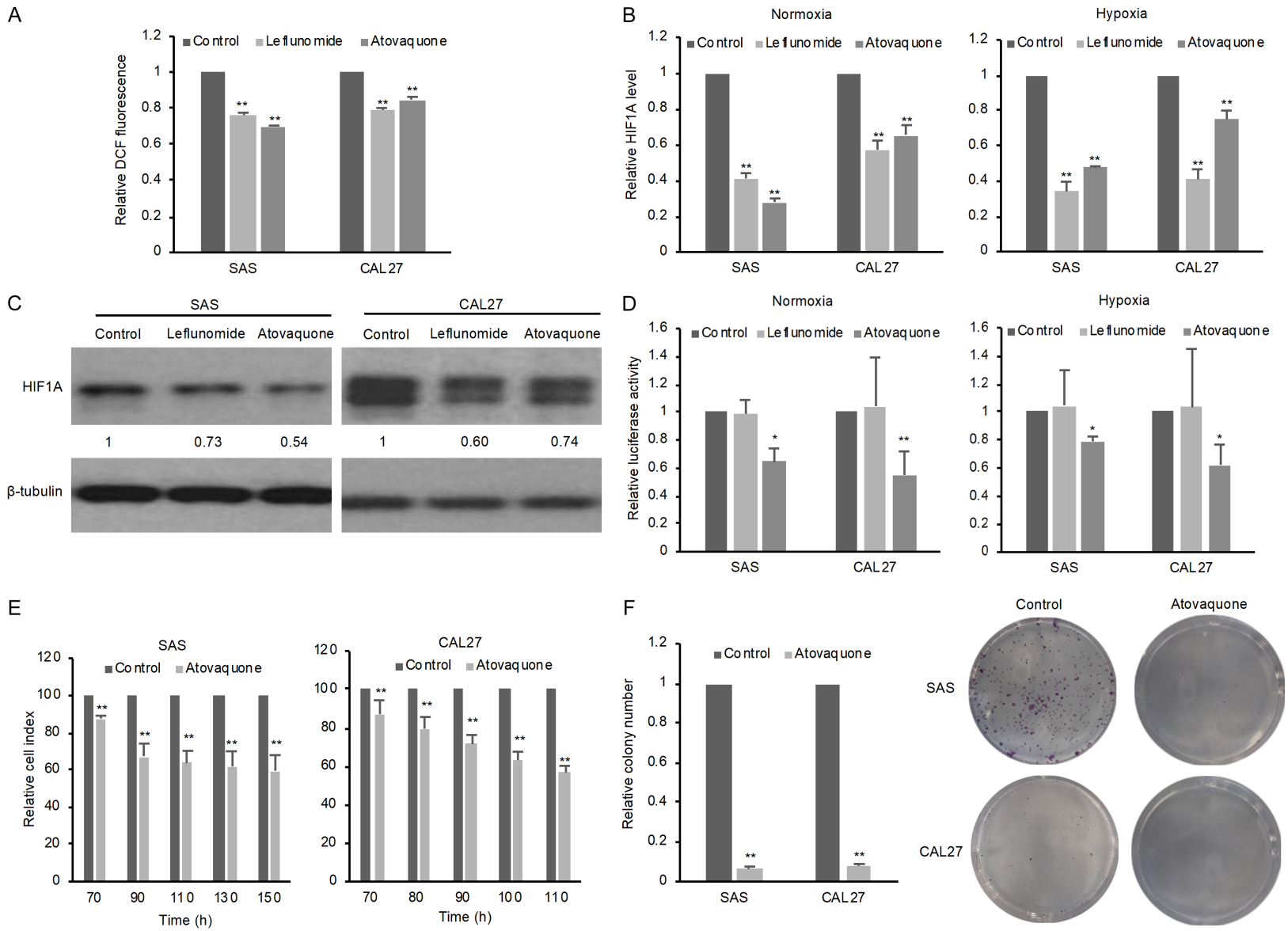
A
Relative DCF fluorescence
Control
Leflunomide
Atovaquone
SAS
CAL27
B
Normoxia
Hypoxia
Relative HIF1A level
C
SAS
CAL27
Control
Leflunomide
Atovaquone
HIF1A
β-tubulin
1
0.73
0.54
1
0.60
0.74
D
Relative luciferase activity
E
Relative cell index
Time (h)
F
Relative colony number
Control
Atovaquone
SAS
CAL27

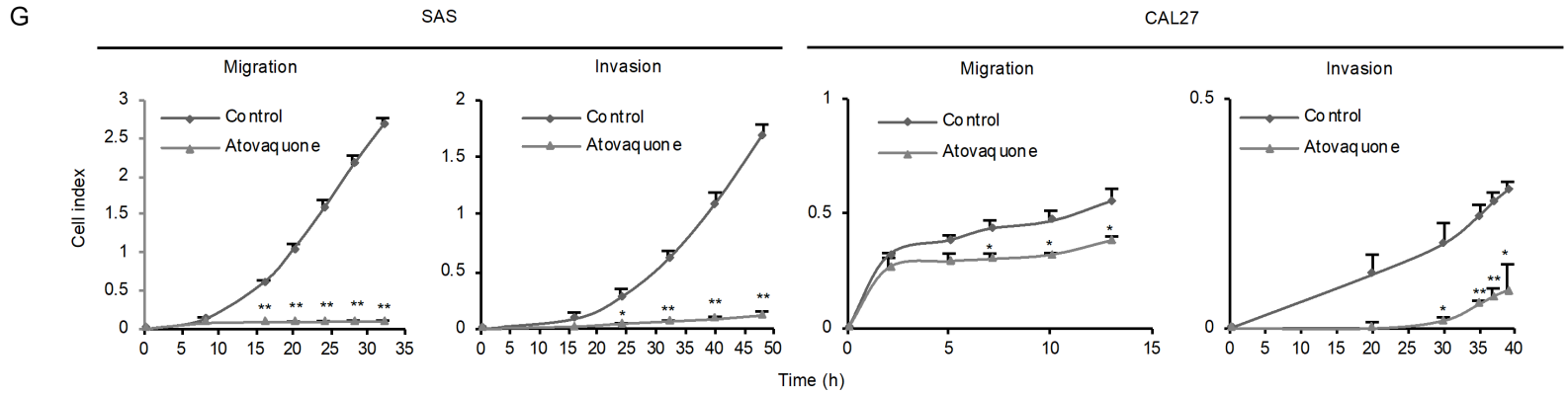

Figure 8. DHODH inhibitors suppressed HIF1A expression and inhibited proliferation, migration and invasion in OTSCC. A. Flow cytometry analysis of intracellular ROS production in OTSCC cells treated with DHODH inhibitors. B. QPCR analysis of HIF1A expression in OTSCC cell treated with DHODH inhibitors. C. Western blot analysis of HIF1A expression in OTSCC cells treated with DHODH inhibitors under hypoxic condition. β-tubulin was used as loading control. Densitometry analysis of bands was carried out using Image Studio™ Lite. Densitometry values of HIF1A were normalized to β-tubulin and displayed under each blot. D. Dual luciferase analysis of transcription activation activity of HIF-1 in OTSCC cells treated with DHODH inhibitors. E. Real-time monitor of proliferation of OTSCC cells treated with atovaquone (15 μM) using xCELLigence DP system. F. Colony formation assay of OTSCC cells treated with atovaquone (10 μM). G. Real-time monitor of cell migration and invasion using xCELLigence DP system in OTSCC cells treated with atovaquone. Except for special mention, CAL27 cells and SAS cells were treated with leflunomide at the concentration of 3.0 μM and 15.6 μM, respectively. CAL27 cells and SAS cells were treated with atovaquone at the concentration of 5.1 μM and 6.7 μM, respectively. Data are expressed as mean ± SD (n=3). $^{*}P<0.05$, $^{**}P<0.01$ (Student t test).

HIF1A production. The transcription activation effect is mediated by the ROS-generating function of DHODH. Apart from inhibition of oral cancer proliferation and colony formation, atovaquone is a potent inhibitor on oral cancer migration and invasion. Thus, targeting DHODH might be considered as a new treatment regime in oral cancer.

Acknowledgements

This work was supported by National Natural Science Foundation of China (#81773136) and Seed Funding of Basic Research from The University of Hong Kong.

Disclosure of conflict of interest

None.

Address correspondence to: Thian-Sze Wong, Department of Surgery, LKS Faculty of Medicine, The University of Hong Kong, 21 Sassoon Road, Pokfulam, Hong Kong, China. Tel: +852-3917-9604; Fax: +852-3917-9634; E-mail: thiansze@gmail.com

References

[1] Tsantoulis PK, Kastrinakis NG, Tourvas AD, Laskaris G and Gorgoulis VG. Advances in the biology of oral cancer. Oral Oncol 2007; 43: 523-534.

[2] Choi SW and Thomson P. Increasing incidence of oral cancer in Hong Kong-who, where...and why? J Oral Pathol Med 2019; 48: 483-490.

[3] Haddad RI and Shin DM. Recent advances in head and neck cancer. N Engl J Med 2008; 359: 1143-1154.

[4] Shield KD, Ferlay J, Jemal A, Sankaranarayanan R, Chaturvedi AK, Bray F and Soerjomataram I. The global incidence of lip, oral cavity, and pharyngeal cancers by subsite in 2012. CA Cancer J Clin 2017; 67: 51-64.

[5] Bredell MG, Ernst J, El-Kochairi I, Dahlem Y, Ikenberg K and Schumann DM. Current relevance of hypoxia in head and neck cancer. Oncotarget 2016; 7: 50781-50804.

[6] Denko NC, Fontana LA, Hudson KM, Sutphin PD, Raychaudhuri S, Altman R and Giaccia AJ. Investigating hypoxic tumor physiology through gene expression patterns. Oncogene 2003; 22: 5907-5914.

[7] Li JN, Feng ZE, Wang L, Wang YX and Guo CB. Expression of hypoxia-inducible factor 1alpha is associated with lymph node metastasis in oral squamous cell carcinoma. Beijing Da Xue Xue Bao Yi Xue Ban 2018; 50: 26-32.

[8] Zhong Z, Zhang H, Hong M, Sun C, Xu Y, Chen X, Gao C, He M, Liu W and Liang J. FNDC3B promotes epithelial-mesenchymal transition in tongue squamous cell carcinoma cells in a hypoxic microenvironment. Oncol Rep 2018; 39: 1853-1859.

[9] Zhou J, Huang S, Wang L, Yuan X, Dong Q, Zhang D and Wang X. Clinical and prognostic significance of HIF-1alpha overexpression in oral squamous cell carcinoma: a meta-analysis. World J Surg Oncol 2017; 15: 104.

[10] Lee LT, Wong YK, Chan MY, Chang KW, Chen SC, Chang CT and Wang J. The correlation between HIF-1alpha and VEGF in oral squamous cell carcinomas: expression patterns and quantitative immunohistochemical analysis. J Chin Med Assoc 2018; 81: 370-375.

[11] de Aquino Martins ARL, Santos HBP, Mafra RP, Nonaka CFW, Souza LB and Pinto LP. Participation of hypoxia-inducible factor-1alpha and lymphangiogenesis in metastatic and non-metastatic lower lip squamous cell carcinoma. J Craniomaxillofac Surg 2018; 46: 1741-1747.

[12] Kesarwala AH, Krishna MC and Mitchell JB. Oxidative stress in oral diseases. Oral Dis 2016; 22: 9-18.

[13] Liu LZ, Hu XW, Xia C, He J, Zhou Q, Shi X, Fang J and Jiang BH. Reactive oxygen species regulate epidermal growth factor-induced vascular endothelial growth factor and hypoxia-inducible factor-1alpha expression through activation of AKT and P70S6K1 in human ovarian cancer cells. Free Radic Biol Med 2006; 41: 1521-1533.

[14] Pialoux V, Mounier R, Brown AD, Steinback CD, Rawling JM and Poulin MJ. Relationship between oxidative stress and HIF-1alpha mRNA during sustained hypoxia in humans. Free Radic Biol Med 2009; 46: 321-326.

[15] Guzy RD and Schumacker PT. Oxygen sensing by mitochondria at complex III: the paradox of increased reactive oxygen species during hypoxia. Exp Physiol 2006; 91: 807-819.

[16] Rawls J, Knecht W, Diekert K, Lill R and Loffler M. Requirements for the mitochondrial import and localization of dihydroorotate dehydrogenase. Eur J Biochem 2000; 267: 2079-2087.

[17] Khutornenko AA, Roudko VV, Chernyak BV, Vartapetian AB, Chumakov PM and Evstafieva AG. Pyrimidine biosynthesis links mitochondrial respiration to the p53 pathway. Proc Natl Acad Sci U S A 2010; 107: 12828-12833.

[18] Fang J, Uchiumi T, Yagi M, Matsumoto S, Amamoto R, Takazaki S, Yamaza H, Nonaka K and Kang D. Dihydro-orotate dehydrogenase is physically associated with the respiratory complex and its loss leads to mitochondrial dysfunction. Biosci Rep 2013; 33: e00021.

[19] Mohamad Fairus AK, Choudhary B, Hosahalli S, Kavitha N and Shatrah O. Dihydroorotate dehydrogenase (DHODH) inhibitors affect ATP depletion, endogenous ROS and mediate S-phase arrest in breast cancer cells. Biochimie 2017; 135: 154-163.
[20] Fofaria NM and Srivastava SK. STAT3 induces anoikis resistance, promotes cell invasion and metastatic potential in pancreatic cancer cells. Carcinogenesis 2015; 36: 142-150.
[21] Dengler VL, Galbraith M and Espinosa JM. Transcriptional regulation by hypoxia inducible factors. Crit Rev Biochem Mol Biol 2014; 49: 1-15.
[22] Hohn T, Corsten S, Rieke S, Muller M and Rothnie H. Methylation of coding region alone inhibits gene expression in plant protoplasts. Proc Natl Acad Sci U S A 1996; 93: 8334-8339.
[23] Hosseini M, Dousset L, Mahfouf W, Serrano-Sanchez M, Redonnet-Vernhet I, Mesli S, Kasraian Z, Obre E, Bonneu M, Claverol S, Vlaski M, Ivanovic Z, Rachidi W, Douki T, Taieb A, Bouzier-Sore AK, Rossignol R and Rezvani HR. Energy metabolism rewiring precedes UVB-induced primary skin tumor formation. Cell Rep 2018; 23: 3621-3634.
[24] Agani FH, Pichiule P, Carlos Chavez J and LaManna JC. Inhibitors of mitochondrial complex I attenuate the accumulation of hypoxia-inducible factor-1 during hypoxia in Hep3B cells. Comp Biochem Physiol A Mol Integr Physiol 2002; 132: 107-109.
[25] Movafagh S, Crook S and Vo K. Regulation of hypoxia-inducible factor-1a by reactive oxygen species: new developments in an old debate. J Cell Biochem 2015; 116: 696-703.
[26] Qutub AA and Popel AS. Reactive oxygen species regulate hypoxia-inducible factor 1alpha differentially in cancer and ischemia. Mol Cell Biol 2008; 28: 5106-5119.
[27] Breedveld FC and Dayer JM. Leflunomide: mode of action in the treatment of rheumatoid arthritis. Ann Rheum Dis 2000; 59: 841-849.
[28] Davis JP, Cain GA, Pitts WJ, Magolda RL and Copeland RA. The immunosuppressive metabolite of leflunomide is a potent inhibitor of human dihydroorotate dehydrogenase. Biochemistry 1996; 35: 1270-1273.
[29] Nixon GL, Moss DM, Shone AE, Lalloo DG, Fisher N, O'Neill PM, Ward SA and Biagini GA. Antimalarial pharmacology and therapeutics of atovaquone. J Antimicrob Chemother 2013; 68: 977-985.
[30] Petersen E. The safety of atovaquone/proguanil in long-term malaria prophylaxis of nonimmune adults. J Travel Med 2003; 10 Suppl 1: S13-15; discussion S21.
[31] Knecht W, Henseling J and Loffler M. Kinetics of inhibition of human and rat dihydroorotate dehydrogenase by atovaquone, lawsone derivatives, brequinar sodium and polyporic acid. Chem Biol Interact 2000; 124: 61-76.